Publ. Astron. Obs. Belgrade No. 107 (2025), 29 - 36 *Invited Lecture*
http://doi.org/10.69646/14sbac04p

SOHO/ERNE PROTON FLUENCE IN SOLAR CYCLES 23 AND 24

R. MITEVA[1], S. W. SAMWEL[2] and M. DECHEV[1]
[1]*Institute of Astronomy and National Astronomical Observatory (IANAO), Bulgarian Academy of Sciences, 1784 Sofia, Bulgaria*
E–mail: rmiteva@nao-rozhen.org
[2]*National Research Institute of Astronomy and Geophysics (NRIAG), Helwan, Cairo 11421, Egypt*

Abstract. The focus of this study is on solar proton events detected by the SOHO/ERNE instrument during solar cycles (SC) 23 and 24. We select the output produced by the first channel of the high energy detector or at about 15 MeV. This report presents the distributions of the onset-to-peak proton fluences, in terms of their strength, location of their solar origin and mutual correlations, well as the SC trends.

1. INTRODUCTION

In the current phase of its evolution, our Sun emits nearly steady amounts of light, heat, and plasma (solar wind). In addition, there are episodes of less or more violent eruptions with variable occurrence. The manifestations of this activity is entirely driven by the changes in the solar magnetic field. The minute-to-month influence of the solar activity in the heliosphere, planetary magnetospheres and atmospheres, technological devices (both in space and on ground) and the health of humans is knows as space weather (Temmer, 2021) and is currently a topic of multidisciplinary research.

Historically, the activity of our star is reflected in the rise and fall of the numbers of sunspots (Arlt and Vaquero 2020, `https://www.sidc.be/SILSO/home`), which are the darker than the surrounding photosphere when observed in white light and places of concentrations of magnetic flux. The roughly 11-year period from the first appearance, via a (double) maximum, to the disappearance of sunspots is known as a solar cycle (SC), Hathaway (2015), and currently the 25th SC is in its maximum phase. The variation of the sunspot number is followed closely by the other manifestations of solar activity, namely, active regions (ARs), solar flares (SFs), coronal mass ejections (CMEs), filament eruptions, solar energetic particles (SEPs), see, e.g., Miteva (2024). Concise definitions are given below:

- ARs: 'The totality of all observable phenomena preceding, accompanying and following the birth of sunspots including radio-, X-, EUV- and particle emission.' (by van Driel-Gesztelyi and Green 2015)

- SFs: can be regraded '...observationally as a brightening of any emission across the electromagnetic spectrum occurring at a time scale of minutes to hours.

Most manifestations seem to be secondary responses to the original energy release process, converting magnetic energy into particle energy, heat, waves, and motion.' (by Benz, 2017)

- CMEs: '...consist of large structures containing plasma and magnetic fields that are expelled from the Sun into the heliosphere.' (by Webb and Howard, 2012)
- Filaments/prominences: Arcade-like structures (i.e. long and thin clouds) suspended in the solar corona but about hundred times cooler and denser than the coronal material (e.g., Parenti, 2014). The former term is used when observing the structure against the bright solar disk, whereas the latter term is used when viewing the phenomena over the solar limb.
- SEPs: Protons, electrons and heavy ions accelerated near the Sun from 'suprathermal (few keV) up to relativistic (few GeV) energies' (Desai and Giacalone, 2016)

The majority of the key players of solar activity extend their (direct or indirect) influence into the heliosphere. The focus of this study, however, is on the solar protons, accelerated in the solar corona or/and interplanetary (IP) space (Klein and Dalla, 2017). The energetic protons are one of the main drivers of space weather effects, due to their risk of radiation exposure to astronauts (Semkova et al. 2018), and electronics onboard spacecraft (Samwel et al., 2019; Zheng et al., 2019). The remaining drivers, namely, the extreme ultraviolet emission during SFs causes disturbances in the terrestrial ionosphere (Buonsanto 1999) and can disrupt the radio signals. Tens of hours to several days later, upon reaching Earth, the IP counterparts of the CMEs, namely ICMEs, can cause geomagnetic disturbances (Lakhina and Tsurutani, 2016). Also, fast streams of the solar wind are nowadays recognized to have space weather consequences, though of lower intensity compared to the ICMEs.

The two main accelerators in the solar corona by the process of magnetic reconnection during SFs, and shocks formed due to ICMEs are nowadays widely recognized as SEP accelerators (Trottet et al., 2015; Klein and Dalla, 2017). Although some researchers tend to split their effects based on the SEP profile, others tend to regard the combined influence of SF with CME to the solar particles. In our analyses, we will assume either driver as plausible and will retain them in the analyses.

There is a large number of former studies that focus on various aspects of the SEP research: time coverage, energy, instrument, observations, modeling, forecasting (Whitman et al., 2023), and thus describing them goes beyond the scope of this report. Below we list several open-access proton catalogs:

- `http://sepem.eu/help/event_ref.html`
- `https://sepserver.eu/`
- `https://umbra.nascom.nasa.gov/SEP/`
- `http://www.stil.bas.bg/SEPcatalog/`
- `https://catalogs.astro.bas.bg/`

whereas the only catalog of solar electron events is available here:

- `https://www.nriag.sci.eg/ace_electron_catalog/`.

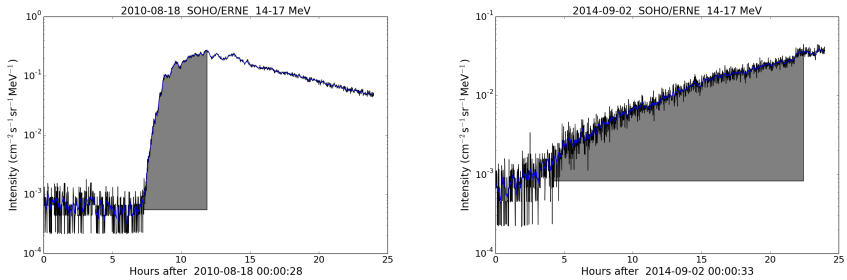

Figure 1: Examples of different time profiles (the fluence is calculated over the shaded area).

2. METHODS

2. 1. PROTON FLUENCE

For the study presented here we use proton data from SOHO/ERNE instrument (Torsti et al. 1995). The complete description on the procedure of proton identification in the SOHO/ERNE high energy detector (HED) data together with the association of their solar origin can be found in Miteva et al. (2024), noted henceforth as Paper I. For this study the proton data is taken from `https://export.srl.utu.fi/` over SCs 23 and 24 (1996−2019).

In contrast to Paper I, here we performed calculations of the onset-to-peak fluences by integration of the time profiles of the proton amplitude (or flux) based on one-day plots. The onset and peak times are identified based on the respective pre-event and peak-time intervals selected by an observer. For this report we use fluences in the first HED channel, namely over the energy range 14−17 (15.5) MeV. It is denoted as $F_{\rm p}$ and the fluence is measured in $(\mathrm{cm}^2\ \mathrm{sr\ MeV})^{-1}$. The value of the proton fluences in all 10 HED energy channels will be made publicly available by us via `https://catalogs.astro.bas.bg/`.

The proton fluence is shown for two examples in Figure 1. Since the definition for the end of a proton event is less objective, we decided to use onset-to-peak proton fluences for the presented below analyses. Nevertheless, depending on whether the event has a fast or a slowly rising profile, the onset-to-peak fluence adopted here covers a different portion of the total event fluence. Based on these limitations, our results can be regarded as representative for the initial phase of the proton event development.

2. 2. SOLAR ERUPTIVE PHENOMENA

The solar origin of the SEP events are adopted from Paper I, based on the following catalogs, which are widely used in solar physics research:

- SFs: `ftp://ftp.swpc.noaa.gov/pub/warehouse/` and `https://solarmonitor.org/` We adopt the reported there SF class, helio-longitude and timing (onset, peak and end).
- CMEs: `https://cdaw.gsfc.nasa.gov/CME_list/` (Gopalswamy et al. 2009). We use the linear (projected) CME speed and angular width (AW) as reported.

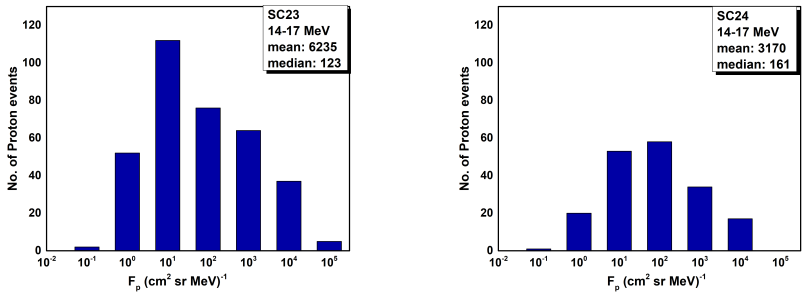

Figure 2: Histograms for the SEP fluence in SC23 (left) and in SC24 (right plot).

3. RESULTS

3. 1. FLUENCE DISTRIBUTION

In total of 664 proton events were identified in HED01 channel in Paper I, however we could calculate the fluence for 475 cases (348 in SC23 and 179 in SC24), due to some data issues for the remaining ones. The distributions of the values for the proton fluences are shown in Figure 2, separately for SC23 (left) and SC24 (on the right).

Over SC23, the peak of the fluence distribution of the 15 MeV protons is at 10 $(\mathrm{cm}^2\ \mathrm{sr\ MeV})^{-1}$ (median value of 123), whereas in SC24 the peak is slightly shifted at 100 $(\mathrm{cm}^2\ \mathrm{sr\ MeV})^{-1}$ (median of 161), with large contribution at the lower bin as well. The mean value for the proton fluence in SC23 is about twice as larger compared to the value in SC24.

3. 2. FLUENCE VS. PEAK INTENSITY

For comparative purpose, we also show the scatter plots between the proton fluence (this study) vs. peak proton intensity (Paper I), see Figure 3. The (double $\log_{10}$) Pearson correlation coefficient $F_\mathrm{p} - J_\mathrm{p}$ in SC23 (top plot) is 0.89±0.02 based on 348 pairs, whereas for SC24 (bottom plot) we obtain nearly the same value for the correlation, 0.87±0.03, over a much smaller number of pairs, 179.

In order to evaluate the statistical uncertainty on a correlation between two sets of data, we use the bootstrapping method (Wall, J.V. and Jenkins, 2003), where out of the original sample are drawn events (with repetitions allowed), by means of a random selection. The 'replica' distribution has the same number of proton events as the original one and its Pearson correlation coefficient is calculated. The procedure is repeated 1000 times and the standard deviation over all (1000) Pearson correlations is adopted as the uncertainty on the correlation of the original sample.

Using this method were obtained the uncertainties on the $F_\mathrm{p} - J_\mathrm{p}$ calculations above, as well as on the correlations between the proton fluence and the solar origin.

3. 3. SOLAR ORIGIN DISTRIBUTIONS

In SC23 the proton-associated SFs range from X28 to B2.3 with mean/median values M9.2/M1.5, whereas in SC24 we obtain a much narrow range in SF class, from

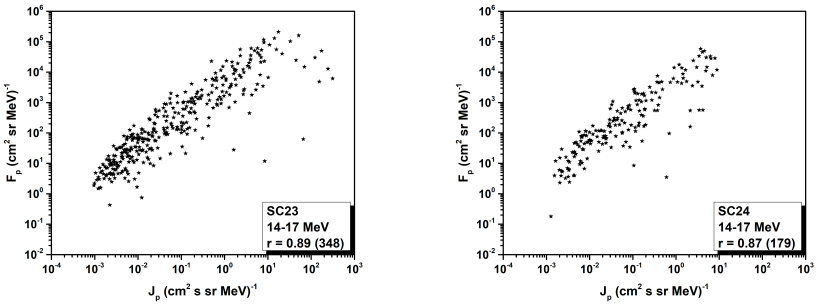

Figure 3: Scatter plots between the SEP fluence and peak intensity in SC23 (left) and in SC24 (on the right).

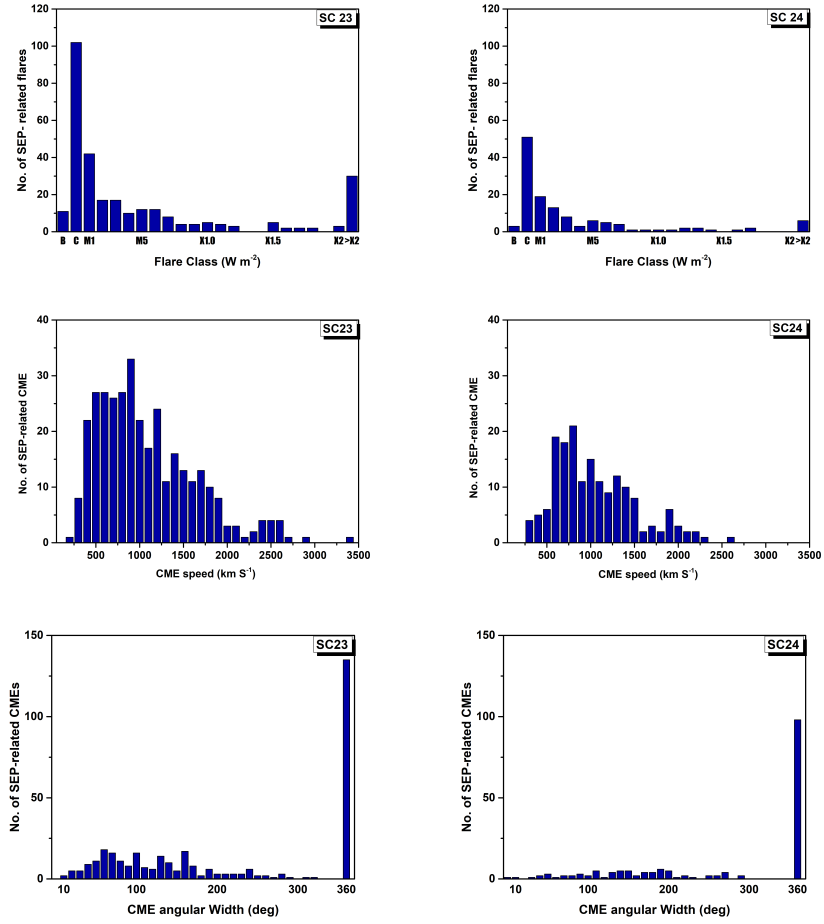

Figure 4: Histograms of the SF class (top) and CME speed (middle) and AW (bottom) for SC23 (left) and SC24 (on the right).

Table 1: Table of the Pearson correlation coefficients in SC23 and SC24 between the proton fluence with the SF class and CME speed, respectively. The event size is given in parentheses.

correlations	SC23	SC24
$F_{\rm p} - I_{\rm SXR}$		
all events	0.50 ± 0.05 (241)	0.40 ± 0.09 (110)
Eastern	0.44 ± 0.09 (56)	0.42 ± 0.17 (31)
Western	0.52 ± 0.06 (180)	0.44 ± 0.10 (79)
strong	0.43 ± 0.07 (134)	0.38 ± 0.04 (61)
weak	0.13 ± 0.11 (107)	0.10 ± 0.15 (49)
$F_{\rm p} - V_{\rm CME}$		
all events	0.51 ± 0.05 (275)	0.48 ± 0.06 (154)
Eastern	0.48 ± 0.11 (59)	0.35 ± 0.15 (42)
Western	0.53 ± 0.05 (216)	0.55 ± 0.07 (112)
strong	0.44 ± 0.07 (148)	0.38 ± 0.09 (80)
weak	0.11 ± 0.08 (127)	0.26 ± 0.10 (74)

X9.3 to B6.2 and weaker mean values compared to SC23, namely M5.4, but slightly stronger in median values, M1.8. The SF class distribution in shown in the top row of Figure 4.

With respect to the SF impulsiveness, in SC23 the SFs are more impulsive, with mean/median rise times (onset-to-peak duration) of 27/17 minutes, whereas in SC24 the SFs show a more gradual rise time, with values 36/23 minutes, correspondingly. With respect to their helio-longutude, we have 56 SFs with Eastern helio-longitudes in SC23 and 31 in SC24. At Western helio-longitudes are located 180 SFs in SC23 and 79 in SC24.

The mean/median values for the CME speeds and AWs are:

- SC23: $\sim$1020/900 km s^{-1}; 218/190 degrees
- SC24: $\sim$980/860 km s^{-1}; 277/360 degrees

indicating faster but narrower proton-associated CMEs in SC23 comparing to SC24. The CME speed distribution in shown in the middle row of Figure 4 with slightly more pronounced tail towards large values. Despite the pronounced peak for halo CMEs (with AW of 360 degrees) both for SC23 and SC24 (bottom row), there is a larger number of narrow CMEs (AW$<$200) in SC23 leading to the lower mean/median values.

3. 4. PEARSON CORRELATIONS

An important evaluation of the influence of the solar origin (SF vs. CME) to the proton intensity or/and fluence is the calculation of Pearson correlations between the values. Here, the correlations are performed between the ($\log_{10}$) proton fluence with the ($\log_{10}$) SF class ($I_{\rm SXR}$) or/and with CME speed ($V_{\rm CME}$), respectively. The results are summarized in Table 1 for different sub-samples of the proton events and separately for SC23 and SC24.

For the entire sample (denoted as 'all events'), we obtain stronger correlations in SC23 compared to SC24, both with the SFs and with the CMEs. Considering the uncertainty ranges, however, the differences are not statistically significant.

Furthermore, the proton sample is divided into Eastern and Western, according to the longitude of their associated SFs or measurement position angle of the associated CMEs. A prevalence of the correlations with protons at Western-origin is obtained, both with SFs and CMEs, and in either SCs. However, due to the lower number of events in the respective samples, the uncertainty ranges are larger and thus there is no statistical significance.

The last division of the proton sample is done according to the median value of the proton fluence (see Figure 2), namely into strong vs. weak. A statistically different correlations with the SFs are obtained between the strong and weak proton events in either SC. Similarly, the correlations between the strong proton fluences and the CMEs have larger values compared to the correlations with the weaker protons, however the difference in SC24 are not statistically significant.

4. SUMMARY

This report presents the first results on the analyses of the 14−17 MeV proton fluences from SOHO/ERNE data in terms of their distribution, cross-correlation with the respective proton peak intensity values and Pearson correlations with the SF class and CME speed. The proton sample is subsequently split into Eastern vs. Western (based on the solar origin helio-location) and strong vs. weak events (based on the median values of the entire fluence sample). Finally, the results are outlined separately for SC23 and SC24 in order to investigate the SC trends. The notable trends are summarized below, both for the SF class and CME speed, though mostly not statistically significant differences are found:

- SC: Overall, the Pearson correlations in SC24 are weaker compared to those in SC23.
- Helio-longitude: The Pearson correlations for the Western sub-sample shows larger values compared to the Eastern sub-sample.
- Fluence-strength: The proton events with stronger (than the median) fluences show higher Pearson correlations compared to the weaker events.

The above trends will be explored for the remaining HED channels and the results will be presented elsewhere. The values of the SOHO/ERNE HED fluences will be released via an open-access database: `https://catalogs.astro.bas.bg/`.

Acknowledgments

This research was supported by SCOSTEP/PRESTO project 'On the relationship between major space weather phenomena in solar cycles 23 and 24'; by the Bulgarian-Egyptian inter-academy project 'On space effects at near Earth environment - from remote observations and in situ forecasting to impacts on satellites' (2022-2024), Bulgarian Academy of Sciences IC-EG/08/2022-2024 and Egyptian Academy of Scientific Research and Technology (ASRT)/NRIAG (ASRT/BAS/2022-2023/10116) and by the Bulgarian-Serbian inter-academy project 'Active Events on The Sun. Catalogs of

Proton Events and Electron Signatures in X-Ray, UV and Radio Diapason. Influence of Collisions on Optical Properties of Dense Hydrogen Plasma.' (2023-2025).

References

Arlt, R., Vaquero, J. M.: 2020, *Living Reviews in Solar Physics*, **17**, article id.1, doi: 10.1007/s41116-020-0023-y

Benz, A. O.: 2017, *Living Reviews in Solar Physics*, **14**, article id. 2, 59 pp., doi: 10.1007/s41116-016-0004-3

Buonsanto, M. J.: 1999, *Space Science Reviews*, **88 (3/4)** 563–601, doi: 10.1023/A:1005107532631

Desai, M. and Giacalone, J.: 2016, *Living Reviews in Solar Physics*, **13**, article id. 3, 132 pp., doi: 10.1007/s41116-016-0002-5

Hathaway, D. H.: 2015, *Living Reviews in Solar Physics*, **12**, article id. 4, 87 pp., doi: 10.1007/lrsp-2015-4

Gopalswamy, N., Yashiro, S., Michalek, G., Stenborg, G., Vourlidas, A., Freeland, S., Howard, R.: 2009, *Earth Moon and Planets*, **104**, 295–313, doi: 10.1007/s11038-008-9282-7

Klein, K.-L.; Dalla, S.: 2017, *Space Science Reviews*, **212 (3–4)**, 1107–1136, doi: 10.1007/s11214-017-0382-4

Lakhina, G. S. and Tsurutani, B. T.: 2016, *Geoscience Letters*, **3**, article number 5, doi: 10.1186/s40562-016-0037-4

Miteva, R.: 2024, *Journal of Physics: Conference Series*, **2794 (1)**, id.012004, 8 pp., doi: 10.1088/1742-6596/2794/1/012004

Miteva, R., Samwel, S. W., Dechev, M.: 2024, *Atmosphere*, **15 (8)**, id.1016, doi: 10.3390/atmos15081016

Parenti, S.: 2014, *Living Reviews in Solar Physics*, **11**, article id. 1, 88 pp., doi: 10.12942/lrsp-2014-1

Samwel, S. W., Abd El-Aziz, E., Garrett, H. B., Hady, A. A., Ibrahim, M., Amin, M. Y.,: 2019, *Advances in Space Research*, **64**, 239–251, doi: 10.1016/j.asr.2019.03.025

Semkova, J., Koleva, R., Benghin, V., Dachev, T., Matviichuk, Y., Tomov, B., Krastev, K., Maltchev, S., Dimitrov, P., Mitrofanov, I., Malahov, A., Golovin, D., Mokrousov, M., Sanin, A., Litvak, M., Kozyrev, A., Tretyakov, V., Nikiforov, S., Vostrukhin, A., Fedosov, F., Grebennikova, N., Zelenyi, L., Shurshakov, V., Drobishev, S.: 2018, *Icarus*, **303**, 53–66, doi: 10.1016/j.icarus.2017.12.034

Temmer, M.: 2021, *Living Reviews in Solar Physics*, **18 (1)**, article id.4, doi: 10.1007/s41116-021-00030-3

Torsti, J., Valtonen, E., Lumme, M., Peltonen, P., Eronen, T., Louhola, M., Riihonen, E., Schultz, G., Teittinen, M., Ahola, K., Holmlund, C., Kelhä, V., Leppälä, K., Ruuska, P., Strömmer, E.: 1995, *Solar Physics*, **162 (1-2)**, 505–531, doi: 10.1007/BF00733438

Trottet, G., Samwel, S., Klein, K.-L. Dudok de Wit, T. and Miteva, R.: 2015, *Solar physics*, **290**, 819–839, doi: 10.1007/s11207-014-0628-1

van Driel-Gesztelyi, L., Green, L. M.: 2015, *Living Reviews in Solar Physics*, **12**, article id. 1, 98 pp., doi: 10.1007/lrsp-2015-1

Wall, J. V., Jenkins, C. R.: 2003, *Practical Statistics for Astronomers*, **3**

Webb, D. F., Howard, T. A.: 2012, *Living Reviews in Solar Physics*, **9**, article id. 3, 83 pp., doi: 10.12942/lrsp-2012-3

Whitman, K., Egeland, R., Richardson, I. G. et al.: 2023, *Advances in Space Research (review)*, **72, (12)**, 5161–5242, doi: 10.1016/j.asr.2022.08.006

Zheng, Y., Ganushkina, N. Y., Jiggens, P., Jun, I., Meier, M., Minow, J. I., O'Brien, T. P., Pitchford, D., Shprits, Y., Tobiska, W. K., Xapsos, M. A., Guild, T. B., Mazur, J. E., Kuznetsova, M. M.: 2019, *Space Weather*, **17**, 1384–1403, doi: 10.1029/2018SW002042